

Experimental demonstration of asymmetric diffraction based on a passive parity-time-symmetric acoustic grating

Yuzhen Yang,^{1,2} Han Jia,^{1,2,3,*} Yafeng Bi,^{1,2} Han Zhao,^{1,2} Jun Yang^{1,2,3,†}

¹ Key Laboratory of Noise and Vibration Research, Institute of Acoustics, Chinese Academy of Sciences, Beijing 100190, People's Republic of China

² University of Chinese Academy of Sciences, Beijing 100049, People's Republic of China

³ State Key Laboratory of Acoustics, Institute of Acoustics, Chinese Academy of Sciences, Beijing 100190, People's Republic of China

Passive parity-time-symmetric medium provides a feasible scheme to investigate non-Hermitian systems experimentally. Here, we design a passive PT -symmetric acoustic grating with a period equal to exact PT -symmetric medium. This treatment enhances the diffraction ability of a passive PT -symmetric grating with more compact modulation. Above all, it eliminates the first-order disturbance of previous design in diffraction grating. Additional cavities and small leaked holes on top plate in a 2D waveguide are used to construct a parity-time-symmetric potential. The combining between additional cavities and leaked holes makes it possible to modulate the real and imaginary parts of refractive index simultaneously. When the real and imaginary parts of refractive index are balanced in modulation, asymmetric diffraction can be observed between a pair of oblique incident waves. This demonstration provides a feasible way to construct passive parity-time-symmetric acoustic medium. It opens new possibilities for further investigation of acoustic wave control in non-Hermitian systems.

*Corresponding author.

hjia@mail.ioa.ac.cn

†Corresponding author.

jyang@mail.ioa.ac.cn

Parity-time (PT) symmetry is a concept arising from Quantum mechanics, which means the invariance of Hamiltonian under parity-time inversion. It was believed that Hermitian Hamiltonian was the guarantee of real spectra corresponding to observable physical quantities. Until 1998, Bender and Boettcher confirmed that non-Hermitian Hamiltonian could still possess real spectra in a complex system with parity-time reflection symmetry [1]. A necessary but not sufficient condition of PT symmetry is $V(\mathbf{r}) = V^*(-\mathbf{r})$. It means that the real part of the Hamiltonian potential is an even function of position, whereas the imaginary part is an odd function. When the complex potential exceeds a threshold, spontaneous breaking can be observed from the unbroken phase to broken phase of PT symmetry [2-5]. The phase transition singularity is called exceptional point, which is one of the most important characteristic of non-Hermitian Hamiltonian.

In recent years, non-Hermitian system with PT -symmetric potential has been widely applied in fields of classic waves because of the similarity between Schrodinger equation and classic wave equation [5-30]. Many unconventional phenomena in optics have been demonstrated, including Bloch oscillation [6, 7], optical isolation [8, 9], unidirectional invisibility or reflectionless effect [10-12], coherent perfect absorption (CPA) and lasing [15-20, 31]. In addition, many interesting acoustic effects of PT symmetry, such as one-way cloak [32], invisible sensing [22] and sound absorption [33], have also drawn much attention. However, previous works mainly pay attention to PT symmetry of 1D waveguides, in which wave propagates along with the direction of modulation. To enhance the practicability and applicability of PT -symmetric system, research on higher dimensional system is an urgent and important task [34-37]. Diffraction grating is a basic device in 2D waveguide, whose physical characteristics of PT symmetry have been discussed in optics [35-37]. Conventional Bragg scattering gratings with only real-part modulation of refractive index offer a pair of opposite wave vectors $\mathbf{q}' = \pm 2k_B \mathbf{r} / r$, where $k_B = \pi / T$ is the wave number on the Bragg condition. However, PT -symmetric gratings offer a unidirectional wave vector at EP, with balanced modulations between real and imaginary parts ($n_r = n_i$). In this letter,

asymmetric diffraction of a passive PT -symmetric acoustic grating has been investigated theoretically and experimentally. At balanced modulation of real and imaginary parts, the $+1^{\text{st}}$ diffraction order with negative incident Bragg angle is much weaker than -1^{st} diffraction order with positive incident angle. Such asymmetric diffraction acoustic grating have potential applications in many fields, such as beam forming, ultrasonic medical imaging, and directional noise reduction.

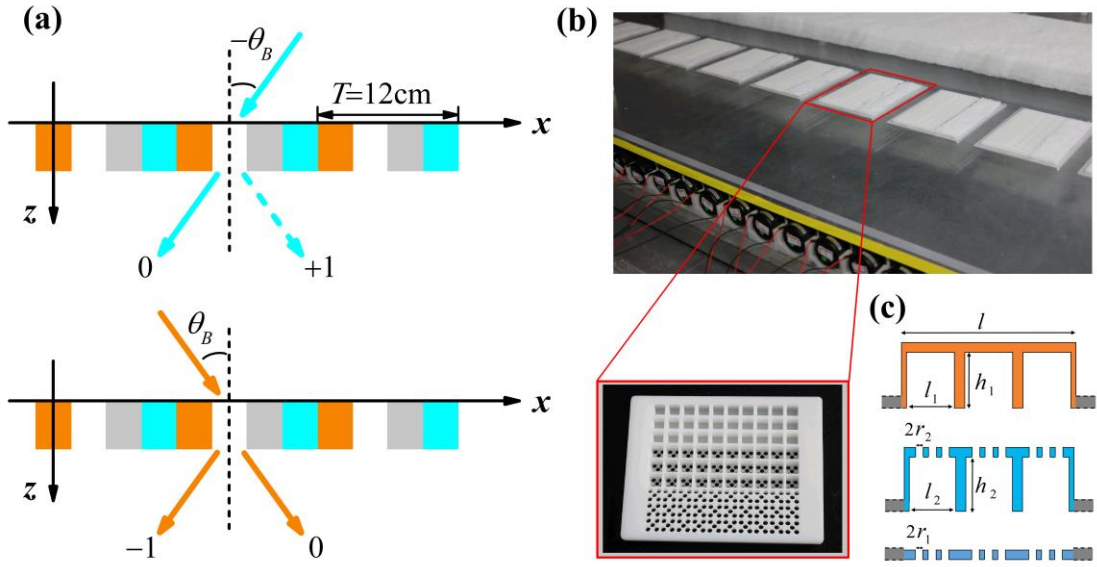


FIG. 1. An asymmetric diffraction grating based on PT -symmetric potential. (a) Upper figure shows diffraction with negative incident angle and lower figure shows diffraction with positive incident angle. The arrows represent incident waves and corresponding diffracted waves. (b) A photo of installation of sample pieces; the picture in red box is the photo of a sample piece fabricated by 3D printing technique. Each sample contains three kinds of modulators side by side. (c) Schematics of three kinds of modulators. The cross-sectional views of modulators for real, superposition of real and imaginary, imaginary parts are displayed from top to bottom. Adopted geometry parameters are $l = 30\text{mm}$, $l_1 = 7.6\text{mm}$, $h_1 = h_2 = 9.0\text{mm}$, $r_1 = 1.7\text{mm}$, $l_2 = 8.6\text{mm}$, and $r_2 = 1.5\text{mm}$, respectively.

In acoustics, PT -symmetric medium can be realized by a complex refractive index obeying the condition $n(\mathbf{r}) = n^*(-\mathbf{r})$. The classic PT -symmetric medium has simple

harmonic modulation of refractive index $n(x) = n_0 + n_r \cos(hx) + in_i \sin(hx)$, where $h = 2\pi/T$ is the reciprocal lattice vector, T is the lattice period, n_0 is the background refractive index and n_r, n_i are the modulation amplitudes of the real and imaginary parts, respectively. The linear acoustic wave equation in the PT -symmetric grating can be written as

$$\Delta P + k_0^2 n^2 P = 0, \quad (1)$$

where $\Delta = \partial^2 / \partial x^2 + \partial^2 / \partial z^2$ is the Laplacian, P is the sound pressure, $k_0 = \omega / c_0$ is the wave number of background medium. The modulation part of the refractive index is given as $n_1(x) = n(x) - n_0$. In a weak coupling regime, the acoustic wave equation can be approximate to

$$\Delta P + k_0^2 (n_0^2 + 2n_0 n_1) P = 0. \quad (2)$$

Here, we focus on the first-order Bragg scattering of the PT -symmetric grating. The high-order diffractions can be negligible in the studied frequency range. The Fourier expansion of the modulated refractive index is $n_1 = C_0 + C_{-1} \exp(ihx) + C_1 \exp(-ihx)$. For the incident monochromatic plane wave at Bragg angle θ_B [$2k \sin(\theta_B) = h$], as shown in Fig. 1(a), the sound pressure in the grating contains two main coupled diffractive waves. A general expression is written as

$$P(\mathbf{r}) = A_0 e^{-i\mathbf{q}_0 \mathbf{r}} + A_h e^{-i\mathbf{q}_h \mathbf{r}}, \quad (3)$$

where A_0, A_h are amplitudes of the zero diffraction order and +1st (-1st) diffraction order, respectively; $\mathbf{q}_0 = (q_{0x}, q_{0z}), \mathbf{q}_h = (q_{hx}, q_{hz})$ are wave vectors of the zero order and +1st (-1st) order diffracted waves in the structure. When the sign of Bragg incident angle is negative, i.e. $-\theta_B$, the relationship between the components of wave vectors can be expressed as $q_{hx} = q_{0x} - h, q_{hz} = q_{0z}$. By substituting Eq. (3) into Eq. (2), we obtain the following coupled-mode equations

$$\begin{cases} (-q_{0x}^2 - q_{0z}^2 + k_0^2 n_0^2 + 2k_0^2 n_0 C_0) A_0 + 2k_0^2 n_0 C_{-1} A_h = 0 \\ 2k_0^2 n_0 C_1 A_0 + (-q_{hx}^2 - q_{hz}^2 + k_0^2 n_0^2 + 2k_0^2 n_0 C_0) A_h = 0 \end{cases}, \quad (4)$$

where $q_{0x} = k_x [k_x = \sin(\theta_B) k_0]$, which follows from Snell's law. The existence of nontrivial solutions of the system expressed by Eq. (4) allows us to write down the dispersion relation for z projections of wave vectors

$$q_{0z}^2 = k_0^2 n_0^2 + 2k_0^2 n_0 C_0 - q_{0x}^2 \pm 2k_0^2 n_0 \sqrt{C_1 C_{-1}}. \quad (5)$$

The two modes of Eq. (5) represent upper and lower deviation of z -directional wave vector due to the periodical modulation of refractive index. Combining Eq. (4) and Eq. (5), the following relationship for the amplitudes of diffractive waves can be obtained:

$$R_{+1} = \frac{A_h}{A_0} = \pm \sqrt{\frac{C_1}{C_{-1}}}, \quad (6)$$

where R_{+1} is the ratio between amplitude coefficients of +1st diffraction order and zero diffraction order. On the other hand, when the sign of the Bragg incident angle changes to positive, i.e. θ_B , relationship between the x -directional projections of wave vectors in the PT -symmetric diffraction grating changes from $q_{hx} = q_{0x} - h$ to $q_{hx} = q_{0x} + h$. As a result, the Fourier coefficients in Eq. (4) exchange between C_1 and C_{-1} . The corresponding diffraction intensity ratio changes to $R_{-1} = A_h / A_0 = \pm \sqrt{C_{-1} / C_1}$ naturally. It can be seen that the diffraction intensity ratios of positive and negative incident angles are both determined by the Fourier coefficients of refractive index. In classic PT -symmetric system, the Fourier coefficients are shown as:

$$C_0^1 = 0, \quad C_1^1 = (n_r - n_i) / 2, \quad C_{-1}^1 = (n_r + n_i) / 2. \quad (7)$$

It is clear that R_{+1} will equal to zero with balanced modulation between real and imaginary parts of refractive index, i.e. $n_r = n_i$, which means the +1st diffraction with negative incident angle will vanish completely at EP.

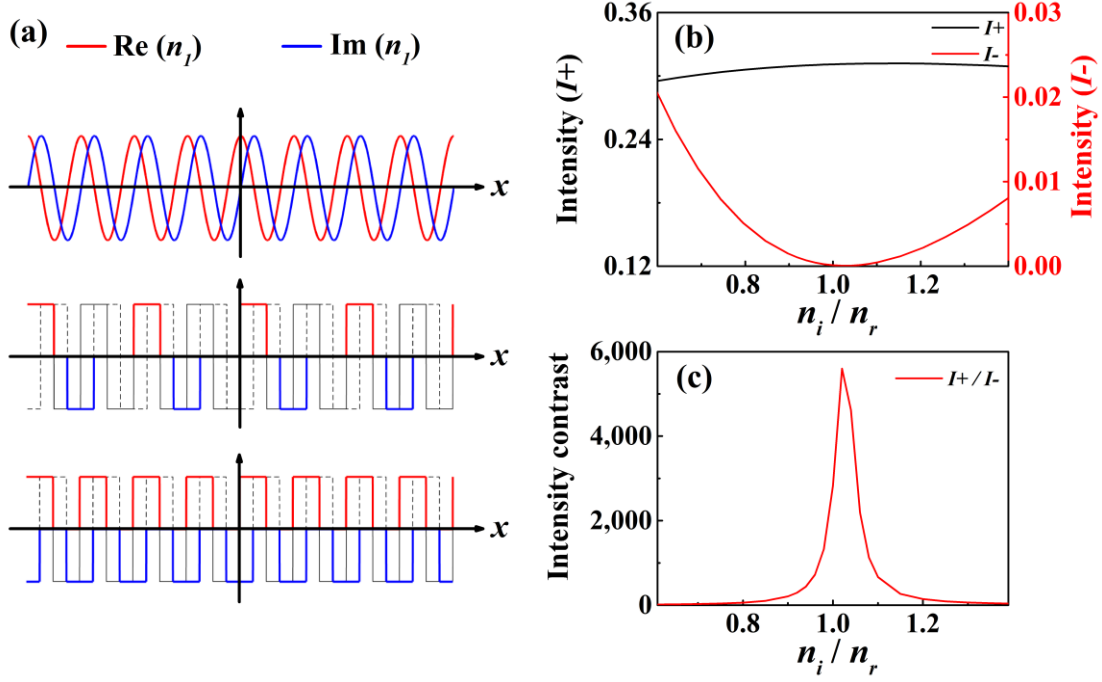


FIG. 2. Evolution of PT -symmetric potential and diffraction characteristic of the revised passive PT -symmetric potential. (a) The modulation of refractive index for exact PT -symmetric medium and passive PT -symmetric mediums. The red (blue) curves denote real (imaginary) part of modulation. The first row represents the modulation of exact PT -symmetric potential. The second row represents the existing popular passive PT -symmetric potential with doubled period. And the third row represents the revised passive PT potential with unchanged period. (b) Diffraction intensity with different modulation ratios. (c) Diffraction intensity ratio between -1^{st} diffraction order and $+1^{\text{st}}$ diffraction order with different modulation ratios.

To simplify the structural design requirement, previous researchers adopted the Fourier translation of a complex square-wave modulation in exchange for the complex exponential modulation. In addition, the manual truncation and in-phase shift of refractive index separate the modulations of real and imaginary parts spatially. Considering the absence of natural gain medium, the gain part is removed to enhance the feasibility of experimental implementations. This evolution process from exact PT -symmetric modulation to passive PT -symmetric modulation is presented in Fig. 2(a). It has been proved that the features at EP of exact PT symmetry can still be observed and controlled in passive PT -symmetric system [11, 34, 37, 38]. However, this adjustment

artificially doubles the modulation period. And the utilization of second-order Bragg scattering will leave unwished first-order disturbance in PT -symmetric diffraction gratings. Moreover, the expansion of the period reduces the ability of diffraction. To overcome the shortage of existing passive PT -symmetric medium in diffraction gratings, we change the period back to that of exact PT -symmetric medium, with overlap of real and imaginary modulations. The Fourier coefficients of refractive indexes in the existing and revised passive PT -symmetric mediums are shown as follows:

$$C_0^2 = \frac{1}{4}(n_r - in_i), \quad C_1^2 = \frac{1}{2\pi}(n_r - n_i), \quad C_{-1}^2 = \frac{1}{2\pi}(n_r + n_i), \quad (8a)$$

$$C_0^3 = \frac{1}{2}(n_r - in_i), \quad C_1^3 = \frac{1}{\pi}(n_r - n_i), \quad C_{-1}^3 = \frac{1}{\pi}(n_r + n_i). \quad (8b)$$

Comparing Fourier coefficients in Eqs. (8) to those of exact PT symmetry in Eq. (7), C_0 is not zero any more for passive PT -symmetric medium due to the absence of gain part. In passive PT -symmetric systems composed by only lossy and lossless parts, the average loss bias can be regarded as the loss of background medium. For both passive PT -symmetric mediums, C_1, C_{-1} still have components of $n_r - n_i$ and $n_r + n_i$, respectively. So asymmetric diffraction effect still keeps valid in these passive PT -symmetric gratings. Moreover, the Fourier coefficients of revised grating are twice of the coefficients of existing PT -symmetric grating, which improve the scattering ability of grating obviously. Above all, the revised Bragg diffraction grating remains no disturbance of other diffraction orders, because the mutual coupling between two main waves in the grating is caused by the first-order Bragg scattering (see Section I of Supplement Material [39]). Diffraction in a revised grating with ideal parameters has been simulated with Comsol Multiphysics. The simulated results are shown in Figs. 2(b) and 2(c). I_+ (I_-) is the sound energy of -1^{st} ($+1^{\text{st}}$) diffraction order with positive (negative) incident angle. From Fig. 2(b), it can be seen that the $+1^{\text{st}}$ diffraction order is suppressed completely at EP, while -1^{st} diffraction order is not very susceptible to the modulation ratio between real and imaginary parts. It is because unidirectional wave vector is generated in the diffraction grating when the modulation reaches the balanced condition

$n_r = n_i$. As long as the modulation deviates from the balanced condition, unidirectional mode coupling will be broken down and +1st diffraction order will appear again. Figure 2(c) shows the intensity contrast between -1st diffraction order and +1st diffraction order with different modulation ratios, which reaches a prominent peak at EP.

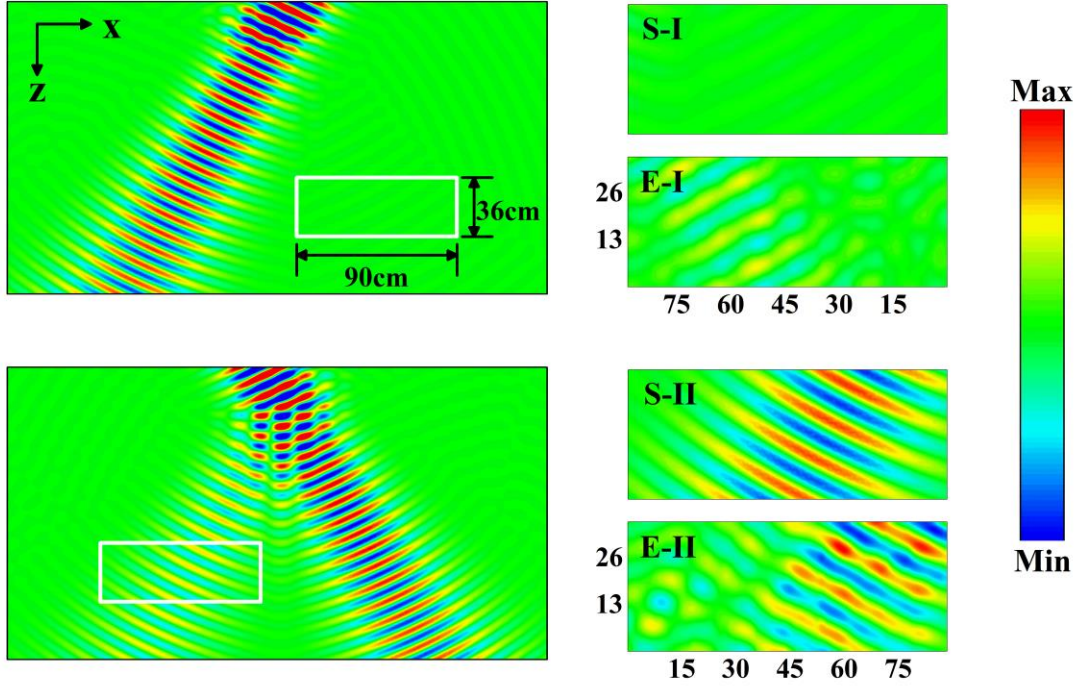


FIG. 3. Asymmetric Bragg diffraction of the revised PT -symmetric acoustic grating at 3.1 kHz. Left column shows the simulated sound pressure fields in the whole 2D waveguide. The +1st diffraction order is suppressed completely (upper figure) while the -1st diffraction order can be observed obviously (lower figure). Corresponding enlarged views of simulated (S-I and S-II) and measured (E-I and E-II) sound pressure fields are shown in right column. Remarkable contrast of different incident angles can be observed in both simulated and measured results.

To verify the asymmetric diffraction effect of the revised passive PT -symmetric grating, we designed an acoustic diffraction grating in a 2D waveguide. In the proposed model, three equal-width parts in a period need to be modulated. The cross-sectional views of corresponding modulators are shown in Fig. 1(c). In this grating, additional upward cavities are selected to modulate the real part and top small holes are chosen to

modulate the imaginary part, similar to the sound leakage of slits [5]. The real and imaginary parts can be modulated simultaneously by combining small holes with additional cavities. Here sound-absorbing cotton is paved on the radiation holes to absorb sound energy as much as possible. Full sound absorption can be obtained with impedance matching boundary condition [40]. The relative impedance of sound-absorbing cotton used here is $1.7+0.1i$ around 3.1 kHz, and the absorption is about 93%. The wanted refractive index distribution can be obtained through adjusting the geometry parameters of modulators, including the height and width of additional cavities and radius of leaked small holes. The adjusting refractive index of three modulators are $n_1^1 = 0.16$, $n_1^2 = 1.03 - 0.16i$, $n_1^3 = 0.17 - 0.15i$, respectively. The modulation parameters endure a little deviation in order to make the retrieval precision meeting the fabrication precision. Three kinds of modulators are arranged side by side to form a sample piece in practical. The period of this grating is $T=12$ cm, and the width of each modulator is 3 cm equaling to $1/4$ period. These samples were fabricated with photosensitive resin via Stereo Lithography Apparatus (SLA) 3D printing technique (0.1mm fabrication precision). In experiment, the waveguide is constructed by two paralleled rigid acrylic plates with a distance of 1.5cm. Ten sample pieces are installed periodically on the top plate to form a diffraction grating, as shown in Fig. 1(b). A loudspeaker array with 24 units is employed to generate a spatial gauss beam. The amplitude and phase of each loudspeaker can be controlled independently through an Antelope sound card with 32-channel output. The sound pressure fields inside the waveguide are scanned using a micro electro-mechanical microphone (Brüel & Kjær 4939), with a spatial resolution of 15 mm. Figure 3 presents the measured sound pressure fields at 3.1 kHz. A simulation with the same working condition as experiment configuration has been implemented for comparison. In the simulation, a pair of oblique incident gauss beams is sent from the top edge of the waveguide. The $+1^{\text{st}}$ order diffraction with negative incident angle is disappeared, while the -1^{st} order with positive incident angle is still observed clearly. The size of measured areas, which are marked by white boxes in the whole waveguide, is 900 mm \times 360 mm. Corresponding enlarged

views of simulated and measured sound pressure fields are shown in right column. The -1^{st} diffraction order is much weaker than $+1^{\text{st}}$ diffraction order in experimental result, which agrees well with simulated result. The asymmetric diffraction deriving from unidirectional wave vector at EP is well demonstrated in the simulated and experimental results.

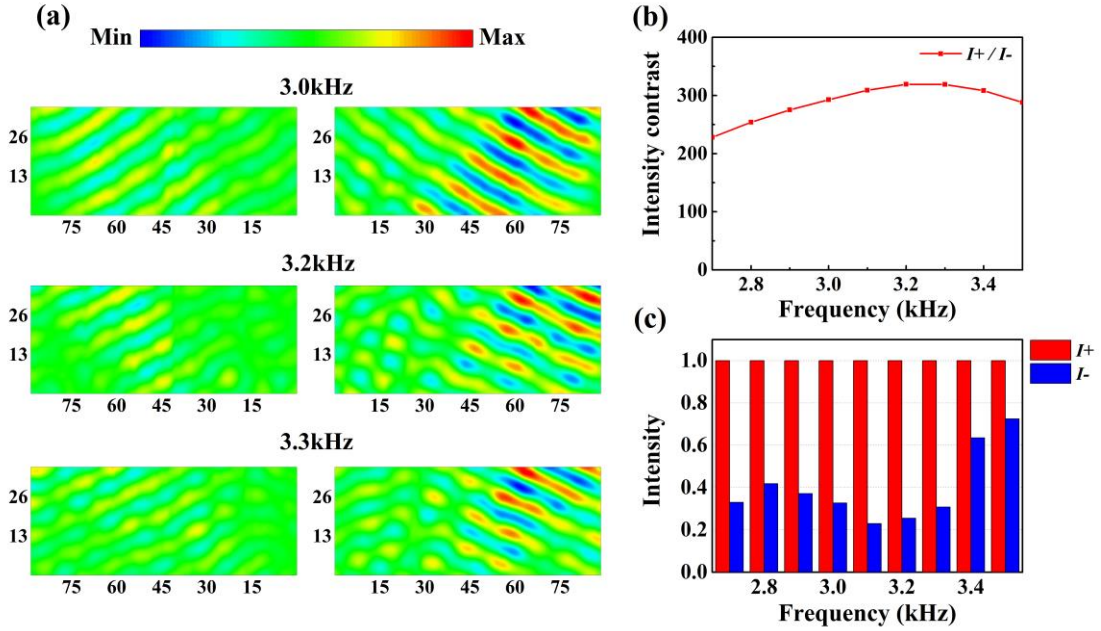


FIG. 4. Asymmetric diffraction phenomenon over a wide frequency range. (a) Measured sound pressure fields of diffracted waves at 3.0 kHz, 3.2 kHz and 3.3 kHz. The $+1^{\text{st}}$ diffraction orders are all much weaker than -1^{st} diffraction orders. (b) The simulated diffraction intensity contrast under the same condition as experiment configuration. (c) Corresponding intensity bars of measured sound fields. The intensity bars of $+1^{\text{st}}$ diffraction order are all lower than those of -1^{st} diffraction order.

The designed passive PT -symmetric grating performs asymmetric diffraction effect in a wide frequency range, since the effective refractive indexes of modulators keep steady in a wide frequency range (see Section II of Supplement Material [39]). The Bragg incident angle will change with different frequencies, as obeying the condition of $2k \sin(\theta_b) = h$. Experimental results of three other frequencies are displayed in Fig. 4(a). From the normalized sound pressure fields, it can be seen that the $+1^{\text{st}}$ diffractions with negative incident angle are much weaker than -1^{st} diffractions

with positive incident angle. In Fig. 4(b), we show the simulated diffraction intensity contrast I^+/I^- with different frequencies, which is higher than 200 in the studied frequency range. Corresponding measured results are displayed in Fig. 4(c). The intensity bars are summations of acoustic energy in the measured areas. It is obvious that the intensity bars of I^- are all much lower than those of I^+ in the measured frequency range. The results of experiment have demonstrated the asymmetric diffraction phenomenon of the designed PT -symmetric grating in a wide frequency range. Theoretically, the $+1^{\text{st}}$ diffraction order should disappear completely at EP. There are some possible reasons for weak signal of $+1^{\text{st}}$ diffraction order, including the fabrication errors of samples, incomplete absorption at the boundary of waveguides.

In conclusion, asymmetric diffraction in a passive PT -symmetric acoustic grating has been achieved experimentally. In this grating, the period of passive PT -symmetric medium is revised to eliminate the first-order disturbance in existing design. A unit combing additional cavities and leaked holes is introduced to modulate the real and imaginary parts of refractive index simultaneously. Asymmetric acoustic gratings provide a feasible way to modulate and control acoustic beams, which may have applications in noise control and beam forming. This study also broadens the route for designing functional PT -symmetric acoustic devices and enables us to investigate further into the physical fundamental of non-Hermitian acoustic systems.

Acknowledgement

This work is supported by the National Natural Science Foundation of China (Grant No. 11874383), the Youth Innovation Promotion Association CAS (Grant No. 2017029), and the IACAS Young Elite Researcher Project (Grant No. QNYC201719).

References:

- [1] C. M. Bender, S. Boettcher, Real Spectra in Non-Hermitian Hamiltonians Having PT Symmetry, *Phys. Rev. Lett.* **80**, 5243 (1998).
- [2] L. Ge, A. D. Stone, Parity-Time Symmetry Breaking beyond One Dimension: The Role of Degeneracy, *Phys. Rev. X* **4**, 031011 (2014).
- [3] A. Guo, G. J. Salamo, D. Duchesne, R. Morandotti, M. Volatier-Ravat, V. Aimez, G. A. Siviloglou, D. N. Christodoulides, Observation of PT -symmetry breaking in complex optical

- potentials, Phys. Rev. Lett. **103**, 093902 (2009).
- [4] P. A. Kalozoumis, C. V. Morfonios, F. K. Diakonou, P. Schmelcher, *PT*-symmetry breaking in waveguides with competing loss-gain pairs, Phys. Rev. A **93**, 063831 (2016).
- [5] C. Shi, M. Dubois, Y. Chen, L. Cheng, H. Ramezani, Y. Wang, X. Zhang, Accessing the exceptional points of parity-time symmetric acoustics, Nat. Commun. **7**, 11110 (2016).
- [6] S. Longhi, Bloch oscillations in complex crystals with *PT* symmetry, Phys. Rev. Lett. **103**, 123601 (2009).
- [7] Y. L. Xu, W. S. Fegadolli, L. Gan, M. H. Lu, X. P. Liu, Z. Y. Li, A. Scherer, Y. F. Chen, Experimental realization of Bloch oscillations in a parity-time synthetic silicon photonic, Nat. Commun. **7**, 11319 (2016).
- [8] L. Chang, X. S. Jiang, S. Y. Hua, C. Yang, J. M. Wen, L. Jiang, G. Y. Li, G. Z. Wang, M. Xiao, Parity-time symmetry and variable optical isolation in active-passive-coupled microresonators, Nat. Photon. **8**, 524 (2014).
- [9] X. Zhou, Y. D. Chong, *PT* symmetry breaking and nonlinear optical isolation in coupled microcavities, Opt. Exp. **24**, 6916 (2016).
- [10] Z. Lin, H. Ramezani, T. Eichelkraut, T. Kottos, H. Cao, D.N. Christodoulides, Unidirectional invisibility induced by *PT*-symmetric periodic structures, Phys. Rev. Lett. **106**, 213901 (2011).
- [11] L. Feng, Y. L. Xu, W. S. Fegadolli, M. H. Lu, J. E. Oliveira, V. R. Almeida, Y. F. Chen, A. Scherer, Experimental demonstration of a unidirectional reflectionless parity-time metamaterial at optical frequencies, Nat. Mater. **12**, 108 (2013).
- [12] V. Achilleos, Y. Auregan, V. Pagneux, Scattering by Finite Periodic *PT*-Symmetric Structures, Phys. Rev. Lett. **119**, 243904 (2017).
- [13] S. Assaworarith, X. Yu, S. Fan, Robust wireless power transfer using a nonlinear parity-time-symmetric circuit, Nature **546**, 387 (2017).
- [14] Y. Auregan, V. Pagneux, *PT*-Symmetric Scattering in Flow Duct Acoustics, Phys. Rev. Lett. **118**, 174301 (2017).
- [15] Y. D. Chong, L. Ge, H. Cao, A. D. Stone, Coherent perfect absorbers: time-reversed lasers, Phys. Rev. Lett. **105**, 053901 (2010).
- [16] Y. D. Chong, L. Ge, A. D. Stone, *PT*-symmetry breaking and laser-absorber modes in optical scattering systems, Phys. Rev. Lett. **106**, 093902 (2011).
- [17] Y. Sun, W. Tan, H. Q. Li, J. Li, H. Chen, Experimental demonstration of a coherent perfect absorber with *PT* phase transition, Phys. Rev. Lett. **112**, 143903 (2014).
- [18] S. Longhi, *PT*-symmetric laser absorber, Phys. Rev. A **82**, 031801(R) (2010).
- [19] L. Feng, Z. J. Wong, R. M. Ma, Y. Wang, X. Zhang, Single-mode laser by parity-time symmetry breaking, Science **346**, 972 (2014).
- [20] H. Hodaei, M. A. Miri, M. Heinrich, D. N. Christodoulides, M. Khajavikhan, Parity-time-symmetric microring lasers, Science **346**, 975 (2014).
- [21] T. Goldzak, A. A. Mailybaev, N. Moiseyev, Light Stops at Exceptional Points, Phys. Rev. Lett. **120**, 013901 (2018).
- [22] R. Fleury, D. Sounas, A. Alu, An invisible acoustic sensor based on parity-time symmetry, Nat. Commun. **6**, 5905 (2015).
- [23] B. Peng, S. K. Oezdemir, F. Lei, F. Monifi, M. Gianfreda, G. L. Long, S. Fan, F. Nori, C. M. Bender, L. Yang, Parity-time-symmetric whispering-gallery microcavities, Nat. Phys. **10**, 394 (2014).

- [24] C. M. Bender, D. C. Brody, H. F. Jones, Complex extension of quantum mechanics, *Phys. Rev. Lett.* **89**, 270401 (2002).
- [25] C. M. Bender, Making sense of non-Hermitian Hamiltonians, *Rep. Prog. Phys.* **70**, 947 (2007).
- [26] K. G. Makris, R. El-Ganainy, D. N. Christodoulides, Z. H. Musslimani, Beam dynamics in PT symmetric optical lattices, *Phys. Rev. Lett.* **100**, 103904 (2008).
- [27] C. E. Rüter, K. G. Makris, R. El-Ganainy, D. N. Christodoulides, M. Segev, D. Kip, Observation of parity–time symmetry in optics, *Nat. Phys.* **6**, 192 (2010).
- [28] A. Regensburger, C. Bersch, M. A. Miri, G. Onishchukov, D. N. Christodoulides, U. Peschel, Parity-time synthetic photonic lattices, *Nature* **488**, 167 (2012).
- [29] S. Longhi, Optical realization of relativistic non-Hermitian quantum mechanics, *Phys. Rev. Lett.* **105**, 013903 (2010).
- [30] J. Christensen, M. Willatzen, V. R. Velasco, M. H. Lu, Parity-Time Synthetic Phononic Media, *Phys. Rev. Lett.* **116**, 207601 (2016).
- [31] P. Bai, K. Ding, G. Wang, J. Luo, Z. Q. Zhang, C. T. Chan, Y. Wu, Y. Lai, Simultaneous realization of a coherent perfect absorber and laser by zero-index media with both gain and loss, *Phys. Rev. A* **94**, 063841 (2016).
- [32] X. Zhu, H. Ramezani, C. Shi, J. Zhu, X. Zhang, PT -Symmetric Acoustics, *Phys. Rev. X* **4**, 031042 (2014).
- [33] V. Achilleos, G. Theocharis, O. Richoux, V. Pagneux, Non-Hermitian acoustic metamaterials: Role of exceptional points in sound absorption, *Phys. Rev. B* **95**, 144303 (2017).
- [34] T. Liu, X. F. Zhu, F. Chen, S. J. Liang, J. Zhu, Unidirectional Wave Vector Manipulation in Two-Dimensional Space with an All Passive Acoustic Parity-Time-Symmetric Metamaterials Crystal, *Phys. Rev. Lett.* **120**, 124502 (2018).
- [35] G. Q. Liang, A. Abouraddy, D. Christodoulides, E. L. Thomas, Asymmetric diffraction from two-component optical gratings made of passive and lossy materials, *Opt. Exp.* **24**, 30164 (2016).
- [36] V. A. Bushuev, L. V. Dergacheva, B. I. Mantsyzov, Asymmetric pendulum effect and transparency change of PT -symmetric photonic crystals under dynamical Bragg diffraction beyond the paraxial approximation, *Phys. Rev. A* **95**, 033843 (2017).
- [37] X. Y. Zhu, Y. L. Xu, Y. Zou, X. C. Sun, C. He, M. H. Lu, X. P. Liu, Y. F. Chen, Asymmetric diffraction based on a passive parity-time grating, *Appl. Phys. Lett.* **109**, 111101 (2016).
- [38] Y. L. Xu, L. Feng, M. H. Lu, Y. F. Chen, Unidirectional Transmission Based on a Passive PT Symmetric Grating With a Nonlinear Silicon Distributed Bragg Reflector Cavity, *IEEE Photon. Journal* **6**, 0600507 (2014).
- [39] See Supplement Material at url for additional simulations, structure design and effective parameters in a wide frequency range.
- [40] M. E. Delany, E. N. Bazley, Acoustical properties of fibrous absorbent materials, *Appl. Acoust.* **3**, 105 (1970).